IOP PUBLISHING JOURNAL OF NEURAL ENGINEERING

J. Neural Eng. **4** (2007) 54–67 doi:10.1088/1741-2560/4/2/006

Conditional firing probabilities in cultured neuronal networks: a stable underlying structure in widely varying spontaneous activity patterns

J le Feber[1], W L C Rutten[1], J Stegenga[1], P S Wolters[2], G J A Ramakers[2] and J van Pelt[2]

[1] Biomedical Signals and Systems/Department of Electrical Engineering, Mathematics, and Computer Science, University of Twente, PO Box 217, 7500AE Enschede, The Netherlands
[2] Netherlands Institute for Neuroscience, Meibergdreef 47, 1105 BA Amsterdam, The Netherlands

E-mail: j.lefeber@utwente.nl

Received 21 July 2006
Accepted for publication 2 January 2007
Published 28 February 2007
Online at stacks.iop.org/JNE/4/54

Abstract

To properly observe induced connectivity changes after training sessions, one needs a network model that describes individual relationships in sufficient detail to enable observation of induced changes and yet reveals some kind of stability in these relationships. We analyzed spontaneous firing activity in dissociated rat cortical networks cultured on multi-electrode arrays by means of the conditional firing probability. For all pairs (i, j) of the 60 electrodes, we calculated conditional firing probability ($CFP_{i,j}[\tau]$) as the probability of an action potential at electrode j at $t = \tau$, given that one was detected at electrode i at $t = 0$. If a $CFP_{i,j}[\tau]$ distribution clearly deviated from a flat one, electrodes i and j were considered to be related. For all related electrode pairs, a function was fitted to the CFP-curve to obtain parameters for 'strength' and 'delay' (i.e. maximum and latency of the maximum of the curve) of each relationship. In young cultures the set of identified relationships changed rather quickly. At 16 days *in vitro* (DIV) 50% of the set changed within 2 days. Beyond 25 DIV this set stabilized: during a week more than 50% of the set remained intact. Most individual relationships developed rather gradually. Moreover, beyond 25 DIV relational strength appeared quite stable, with coefficients of variation (100 × SD/mean) around 25% in periods of ≈10 h. CFP analysis provides a robust method to describe the underlying probabilistic structure of highly varying spontaneous activity in cultured cortical networks. It may offer a suitable basis for plasticity studies, in the case of changes in the probabilistic structure. CFP analysis monitors all pairs of electrodes instead of just a selected one. Still, it is likely to describe the network in sufficient detail to detect subtle changes in individual relationships.

1. Introduction

Over the years, learning and memory have been and still are key topics in brain research. The brain consists of a huge number of neurons that form networks through a multitude of synaptic connections. These networks support a rich repertoire of patterns of electrical activity including uncorrelated and highly synchronized activity. The formation and development of connections is assumed to be crucial in the process of learning, their conservation is assumed to be essential for memory. To demonstrate either memory or learning, one needs to monitor the connections in neuronal networks. Assuming that the specificity of connections is reflected in the patterns of electrical activity in the network, this requires simultaneous measurement of activity in a large number of neurons. *In vivo* this is quite a complicated procedure and several groups now

use *in vitro* preparations of cultured cortical or hippocampal neurons grown over a multi-electrode array (MEA), to enable simultaneous measurement from a large number of neurons (Jimbo *et al* 1998, 1999, 2000, Jimbo and Robinson 2000, Shahaf and Marom 2001, Tal *et al* 2001, Eytan *et al* 2003, 2004, van Pelt *et al* 2004a, 2004b, Ruaro *et al* 2005, Wagenaar *et al* 2006, Chiappalone *et al* 2006).

Cultured dissociated cortical neurons develop into networks that usually become spontaneously active after about a week *in vitro*. The spontaneous activity shows alternating periods of seemingly uncorrelated firing and of synchronized firing, typically growing toward network bursts (Gross *et al* 1995, van Pelt *et al* 2004b). Spontaneous activity, and especially the spatial structure in network burst patterns, have been related to connectivity, and to development of cultured networks when these burst patterns show slow but significant changes (Tateno *et al* 2002, van Pelt *et al* 2004a, 2004b).

Simulation studies suggested that such networks may also be characterized by 'functional connections' between pairs of neurons: abstract representations of possibly parallel neuronal pathways (Aertsen and Gerstein 1985, Melssen and Epping 1987). Various techniques have been developed to identify such connections, most of which are based on or related to cross-correlation analysis (Aertsen and Gerstein 1985, Melssen and Epping 1987, Palm *et al* 1988, Brody 1999, Tam 2001, Castellone *et al* 2003, Chiappalone *et al* 2006). Usually neural activity is modeled by a point process, in which the shape of action potentials is assumed constant and not taken into account.

Identification of neuronal connections is necessary in plasticity studies that aim to investigate changes in connectivity. Recent studies have indicated that cultures of cortical neurons show some kind of plasticity (Jimbo *et al* 1998, 1999, Shahaf and Marom 2001, Marom and Shahaf 2002, Marom and Eytan 2004, Ruaro *et al* 2005), which is necessary to enable learning. On the other hand, stability in connections is important in order to remember what was learned. Different methods were used to induce changes in connectivity. All of these methods were based on the hypothesis that certain patterns of network activity may alter connectivity. In training sessions certain patterns of activity were imposed by electrical stimulation of the network, aiming to induce connectivity alterations.

Cultured cortical networks exhibit spontaneous activity, often in network bursts, which may greatly interfere with the (stimulus induced) changes in certain network connections. Network bursts may contain many action potentials, often far more than the activity induced by electrical stimulation in training sessions, such that their effect on connectivity can be substantial as well.

It is possible to abolish network bursts pharmacologically (Gross *et al* 1995, 1997) or electrically (Wagenaar *et al* 2005b) to avoid this interference. Another approach may be to use network bursts to obtain information about network connectivity. In this latter approach, changes induced in plasticity studies should be detectable, which is often difficult because spontaneous activity may vary in a wide range. The analysis should reveal some kind of stable underlying structure, to enable detection of (subtle but) structural changes. In this approach it is not sufficient to solely observe a selected connection. Recent studies showed that tetanus-induced plasticity is better revealed by patterns of activity in the whole network than by individual responses to test stimuli (Madhavan *et al* 2005, Ruaro *et al* 2005). It seems that cultures of cortical neurons develop an overall balance between connectivity and activity. Such a balance can be disturbed by local tetanization, which drives the network to a new balance. This new balance may or may not support a certain connection that was selected for manipulation and observation.

To properly observe induced connectivity changes after training sessions, one needs a network model that should reveal some kind of stability in individual relationships between electrodes, and describe these relationships in sufficient detail to enable observation of induced changes. Furthermore, connectivity should be monitored in the whole network instead of just one connection.

In this paper we will introduce the conditional firing probability as a measure to describe relationships between pairs of electrodes. Its applicability is tested on sets of data obtained from multi-electrode recordings of spontaneous firing activity in dissociated cultures of rat cortical networks.

We define the conditional firing probability ($\mathrm{CFP}_{i,j}[\tau]$) as the probability that electrode j records a spike at $t = \tau$, given that an action potential was recorded at electrode i at $t = 0$. This approach has also been followed by Marom and Eytan (2004) and Eytan *et al* (2004), who referred to this measure as functional association strength; an abstraction of the biological situation, in which several pathways may be present between each pair of electrodes.

We will develop a matrix description of the relationships between all pairs of active electrodes, based on conditional firing probabilities. Relationships will be characterized by two parameters: the maximum probability will be interpreted as the strength of the relationship, and the latency of this maximum as a measure for propagation time.

In the methods section we will show that CFP is a cross-correlation related measure, calculated from two simultaneously recorded time series of action potential events. Cross-correlation is a non-parametrical technique that describes systems' input/output properties without a predefined model. One of the disadvantages of non-parametric models in general is the lack of parsimony of representation, which complicates interpretation of the model. In our approach, however, the conditional firing probability is interpretable, because it provides relationships between pairs of electrodes, expressed in terms of strength and delay.

2. Materials and methods

2.1. Cell cultures/measurements

Data were obtained from nine cultures: five were measured at University of Twente (UT), and four at Netherlands Institute for Neurosciences (NIN).

At UT, cortical cells were obtained from newborn Wistar rats (four cultures) or from an E18 fetus (one

culture). After trypsin treatment cells were dissociated by trituration. About 400 000 dissociated neurons (400 μl suspension) were plated on an MEA in a 10 mm round spot (precoated with poly ethylene imide). The ring around this spot was removed after 2–3 h. This procedure resulted in a cell density of approximately 5000 cells per mm^2, immediately after plating. On each MEA we counted the number of cells in a randomly chosen 200 $\times$ 200 μm area between four electrodes to confirm this initial cell density.

Neurons were cultured in a circular chamber (inner diameter: 20 mm) glued on top of the MEA. The culture chamber was filled with 700 μl serum-free R12 medium. MEAs were stored in an incubator, under standard conditions of 37 °C, 100% humidity, and 5% CO_2 in air. For recording, we firmly sealed the culture chambers with parafilm and placed the cultures in a measurement setup outside the incubator. In two cultures continuous recordings of several hours were made on a single day. These recordings will be referred to as *single day recordings*. Activity in culture *A* was recorded for 6 h at 12 days *in vitro* (DIV); culture *B* was observed for 10 h at 8 DIV. In three cultures (*C*, *D* and *E*) recordings were started around the 11th day *in vitro*, and lasted for 2 h every day (*daily recordings*). All recordings were started after an accommodation period of at least 20 min. After the measurements the cultures were returned to the incubator.

Data sets recorded at NIN (four rats) have been used before for burst analysis in a study by van Pelt *et al*, for details about the preparation of the cultures see van Pelt *et al* (2004b). In short, dissociated cortical cells obtained from Wistar rat fetuses (E18) were grown over an MEA and kept in culture in a glia conditioned medium. Cell densities were around 5000 cells mm^{-2}. Spontaneous activity in three cultures was recorded almost continuously from the beginning of the second week. In one culture recording was started after 13 days (these data will be referred to as *long-term recordings*).

2.2. Data acquisition

At UT, signals were recorded simultaneously from 60 electrodes (Multi Channel Systems standard MEA; diameter: 10 μm; electrode spacing: 100 μm). After amplification (1000$\times$) and band-pass filtering (10 Hz–6 kHz) all signals were read into a computer at a sample rate of 16 kHz. Noise levels were determined continuously for each channel. A possible spike was detected if a signal crossed a threshold of six times the (rms) noise level. For all threshold crossings a time stamp and electrode number were stored, as well as the waveform. Waveforms were used to eliminate artifacts off-line. Only threshold crossings that belonged to action potential shaped waveforms were included for analysis. We adopted a spike validation technique described by Wagenaar *et al* (2005a).

At NIN 61 electrodes (diameter 12 μm, 70 μm apart) were recorded. An action potential was detected if the signal at an electrode crossed a preset, regularly updated discriminator level. Time stamps were stored with 100 μs precision, corresponding to an effective sample frequency of 10 kHz (technical details have been described in van Pelt *et al* (2004b)). In NIN data it was made plausible that the spike detection procedure resulted in recorded spike trains originating predominantly from single units (neurons) (van Pelt *et al* 2004b). Yet, in this paper we will refer to electrodes, rather than to neurons.

2.3. Data analysis

Connectivity may change with time as new synapses are formed, or it may be altered by changing synaptic efficacies, induced by (certain patterns of) electrical activity in the network. To study the stability of connectivity, one may divide long-term recordings into periods (units) of fixed duration to exclude stability variation caused by varying time spans. In this approach the amount of activity may vary widely between units. This means that in units with relatively few action potentials some connections, and thus also connectivity changes may remain undetected, while units with a very high amount of activity may show much larger changes in connectivity.

Alternatively, long-term recordings may be divided into units that contain a fixed number of action potentials (events), summed over all electrodes. This carries the disadvantage that units may vary in duration, introducing an unwanted possible source of stability variation. However, if we compare the duration of the units afterwards, we may still get an impression of the possible effects of length differences between analysis intervals. We chose to divide recordings into units that contained a fixed number of events. An event consisted of one action potential, or occasionally more than one (simultaneously measured at different electrodes). Data were analyzed in blocks of 2^{15} (= 32 768) events (summed over all electrodes, on average more than 500 events per electrode). This number of events was chosen such that a fair number of electrode pairs recorded enough action potentials to enable statistical analysis of their relationship, while the time resolution (the number of data blocks per unit of time) was still acceptable.

An electrode was considered active if it showed more than 250 action potentials in a data block. At this threshold the number of data points was usually high enough to fit equation (5) (see below), while it was low enough to yield a fair number of active electrodes. In each data block we investigated all possible pairs of active electrodes i and j. We calculated the conditional firing probability ($CFP_{i,j}[\tau]$) as the probability of an action potential at electrode j in the time interval $t = [\tau, \tau + 0.5]$ ($0 \leqslant \tau \leqslant 500$ ms), given that a spike was recorded at electrode i at $t = 0$.

To analyze the measured signals, binary arrays X_i were constructed for all sites $i = 1, \ldots, 60$, with as many data points as the original sampled signals, with $X_i[n] = 1$ at a detected action potential at site i and $X_i[n] = 0$ elsewhere.

The number of action potentials at electrode i that is followed by a spike at j with a delay τ ($N_{\text{follow}_{i,j}}[\tau]$) is now calculated as

$$N_{\text{follow}_{i,j}}[\tau] = \sum X_i[t] \cdot X_j[t + \tau]. \qquad (1)$$

All spikes in 0.5 ms intervals were binned. Equation (1) holds because it is applied to binary arrays X_i and X_j, with $X_{i,j}[n] \in$

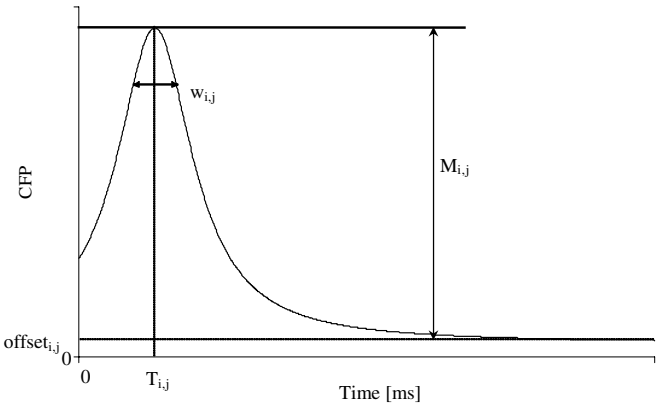

Figure 1. Schematic drawing of the function used to fit conditional firing probability of an electrode pair (i, j) (equation (5)): $M_{i,j}$: maximum probability above offset; $T_{i,j}$: delay at which maximum CFP occurs; $w_{i,j}$: width at offset$_{i,j} + 0.8M_{i,j}$; offset$_{i,j}$ refers to background noise and unrelated background activity.

$\{0, 1\}$ for all n. CFP$[\tau]$ can be calculated by dividing $N_{\text{follow}}[\tau]$ by the total number of action potentials at electrode i (N_i):

$$\text{CFP}_{i,j}[\tau] = \frac{N_{\text{follow}_{i,j}}}{N_i} = \frac{\sum_t X_i[t] \cdot X_j[t+\tau]}{\sum_t X_i[t]} \Bigg| 0 < \tau \leqslant 500 \text{ ms}. \quad (2)$$

CFP$_{i,j}[\tau]$ was calculated for τ equal to multiples of 0.5 ms between 0 and 500 ms. It may be noted that CFP$_{i,j}[\tau]$ is a measure related to cross-correlation ($R_{i,j}[\tau]$):

$$R_{i,j}[\tau] = \frac{1}{L} \sum_{t=1}^{L} X_i[t] \cdot X_j[t+\tau], \quad (3)$$

where L is the length (the number of elements) of the interval in which X_i and X_j are compared.

Thus

$$\text{CFP}_{i,j}[\tau] = \frac{R_{i,j}[\tau]}{\mu_i}, \quad (4)$$

where μ_i ($= 1/L\ \Sigma X_i$) equals the average of X_i, which is proportional to the number of action potentials recorded at electrode i in the interval of length L.

CFP curves were fitted by equation (5) using a Nelder–Mead simplex algorithm (Nelder and Mead 1965) to minimize the mean squared error.

$$\text{CFP}^{\text{fit}}_{i,j}[\tau] = \frac{M_{i,j}}{1 + \left(\frac{\tau - T_{i,j}}{w_{i,j}}\right)^2} + \text{offset}_{i,j} \quad (5)$$

where $M_{i,j}$ is the maximum above offset and $T_{i,j}$ is the delay at which the CFP$^{\text{fit}}$ function reaches its maximum value. Parameter $w_{i,j}$ determines the shape of the curve (the width at 80% of the maximum above offset) and offset$_{i,j}$ reflects unrelated background activity. The choice for this specific function, which is schematically drawn in figure 1, is further discussed in the appendix. In the fit procedure no negative values were allowed for $T_{i,j}$. $M_{i,j}$ was interpreted as a measure for relational strength, $T_{i,j}$ as a measure for latency.

A pair of electrodes was considered related if the shape of the CFP$^{\text{fit}}$ function differed clearly from a flat distribution: $M_{i,j}$ should exceed offset$_{i,j}$ (i.e. the peak CFP$^{\text{fit}}$ value should be larger than twice the offset level) and $w_{i,j}$ should be less than 250 ms (to exclude curves that decreased mainly outside the analysis interval). Furthermore, two exclusion criteria were added based on visual inspection of the fitted lines: $w_{i,j}$ had to be larger than 10 ms to exclude fitting to a single outlying value, and $T_{i,j}$ should not exceed 250 ms. (Approximately 0.1% of all observed relationships showed $T_{i,j} \geqslant 250$ ms, mostly caused by two or three 'responses' in the 500 ms analysis interval that occurred relatively close to each other.) These exclusion criteria led to less than 1% misfits in a test set of 500 fits. All other relationships were fitted without visual inspection.

For all related pairs, values were calculated for $M_{i,j}$ and $T_{i,j}$. The matrices M and T, containing the parameters $M_{i,j}$ and $T_{i,j}$ for all pairs (i, j) of electrodes, gave an overview of all relationships in the network in terms of strength and delay. We calculated M and T for each data block in all cultures. Development of M and T gave insight in the stability of the relationships in the networks. We investigated the stability of the set of identified relationships and the stability of relational strength and delay using either a balanced sample test or continuous stability assessment (see below). Furthermore, we observed the development of individual relationships throughout long-term recordings.

2.4. Stability of set of relationships

First we investigated how quickly the set of identified relationships changed during certain stages in the development of a culture.

Let N be the number of relationships found in a data block (equation (6)).

$$N = |\{M_{i,j} \neq 0\}| = |\{M \neq 0\}|. \quad (6)$$

Here $\{M_{i,j} \neq 0\}$ is the set of electrode pairs (i, j) with non-zero values in M. For readability we will use the notation $\{M \neq 0\}$ for this set of pairs. $|\{M \neq 0\}|$ is the cardinality of the set (the number of non-zero elements in M). Similarity indices (Si) between two matrices M_A and M_B were calculated using equation (7):

$$\text{Si} = \sqrt{\frac{|\{M_A \neq 0\} \cap \{M_B \neq 0\}|^2}{|\{M_A \neq 0\}| \cdot |\{M_B \neq 0\}|}} \quad (7)$$

where $|\{M_A \neq 0\} \cap \{M_B \neq 0\}|$ is the number of pairs that have non-zero value in both M_A and M_B.

Stability of the set of relationships was investigated around reference data blocks at different stages of development (e.g. 16 DIV and 27 DIV in figure 5). For all data blocks we calculated Si with these reference blocks. The development of Si over time indicated how quickly existing relationships disappeared and/or new relationships appeared. For each reference block we calculated an Si curve, which was smoothed using a moving average filter to highlight longer-term trends. The filter averaged each point of the curve with its five neighbors on both sides. From these smooth curves we estimated the interval in which Si did not decrease below 50%. We called this interval int50. For each culture we averaged int50 per day to enable comparison between cultures. We used

mean int50 of all cultures to obtain a measure for the stability of the set of relations.

The development of Si depended only on the existence of relationships and did not take into account the estimated strength ($M_{i,j}$) and delay ($T_{i,j}$) of relationships in the set.

2.5. Stability of relational strength and delay

In the *single day recordings*, we investigated the variability of $M_{i,j}$ and $T_{i,j}$ of all relations that were found in at least 50% of the data blocks. We calculated the coefficient of variation ($\mathrm{CV} = 100 \times \mathrm{SD\ mean}^{-1}$) for each relation in the selected set over all data blocks in which that relation was found. The average CV provided a measure for the mean stability of $M_{i,j}$ (CV_M) and $T_{i,j}$ (CV_T).

2.5.1. Balanced sample test. From each set of *daily recordings*, two days were selected with comparable block lengths. The same group of relationships was selected and again CV_M and CV_T were calculated to compare different stages of development.

To investigate the stability of $M_{i,j}$ and $T_{i,j}$ of the relationships *in long-term recordings*, we examined all data blocks in measurement periods of ≈24 h, collected around 14 DIV or 26 DIV. Two days were selected in which data blocks were of comparable duration. The restriction of balanced samples hampered comparison of different cultures at the exact same days. Again CV_M and CV_T were calculated using all relationships that were found in at least 50% of the data blocks on that day.

2.5.2. Continuous stability assessment. To obtain a more extensive overview of the stability of identified relationships in the network we divided the long-term recording into series of 15 consecutive data blocks (which had a fixed number of action potential events, but varied in duration). For each relationship that was found in at least eight data blocks, we calculated the coefficient of variation. Coefficients of variation were averaged over all relationships in each series of data blocks. This gave an impression of the average stability during such a series. The outcome was plotted against the average of the time interval of each series. To verify that we analyzed a substantial part of all relationships, we calculated the size of the used set as a fraction of all relations that were identified at least twice within a series (thus enabling calculation of SD).

2.6. Development of relationships throughout long-term recordings

Often, electrode pairs were related in many data blocks. We used a set of frequently found relationships to examine the development of relational strength for extended periods of monotonous increase or decrease. A threshold was set to 1 day, and periods (⩾1 day) of increase or decrease should contain at least ten data blocks with the selected relationship. Usually periods of this length also contained some data blocks where the selected relationship was not found because one or both electrodes did not reach the threshold of 250 spikes in that block. These data blocks were not taken into account in this analysis.

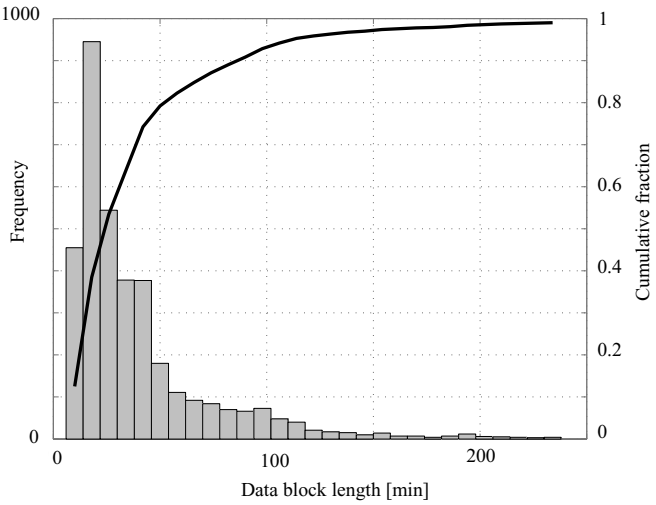

Figure 2. Distribution histogram (left axis) and cumulative fraction (right axis) of data block lengths of all cultures. A data block contains a fixed number of 32 768 spikes, summed over all electrodes. In total 3635 data blocks were analyzed. The distribution shows a mode of 18 min (mean: 46 min). 80% of all data blocks extended over an interval between 10 and 50 min. Data blocks longer than 100 min were mainly found in culture *II* (which showed longer data blocks in general), and in some of the early recordings (up to 17 DIV) in other cultures. Occasionally there were some data blocks longer than 4 h (maximum: 32 h), which were mostly recorded in very young cultures (8–14 DIV) and a few in later recordings of culture *II*. These very long blocks contributed less than 1% to the total number of data blocks and are not shown in the histogram.

Because the networks appeared stable beyond 30 DIV, we selected a set of relationships that were found in at least 50% of all data blocks recorded beyond 30 DIV. We focused on this set to monitor the development of $M_{i,j}$ and $T_{i,j}$ of individual relationships throughout long-term recordings.

3. Results

Data were obtained from nine cultured cortical networks prepared from nine different rats. Recordings lasted either *single day* (cultures *A* and *B*), *daily* (*C*, *D*, and *E*) or *long term* (*I*, *II*, *III*, and *IV*) and started after 8–14 DIV.

Data were analyzed in blocks of 2^{15} (≈33 000) action potential events. In culture *E* (*daily recordings*) none of the two hour measurement periods yielded enough events to fill a single data block. This culture was excluded from further analysis. In the other cultures 80% of the data blocks lasted 10–50 min. Figure 2 shows the distribution of the duration of data blocks.

In each data block conditional firing probabilities ($\mathrm{CFP}_{i,j}[\tau]$) were calculated for all combinations of active electrode pairs (i, j), for $0 \leqslant \tau \leqslant 500$ ms. A typical example of such a CFP graph is shown in figure 3, as well as the parameters obtained by fitting equation (5).

The vast majority of CFP curves could be fitted adequately by equation (5). However, occasionally a probably present

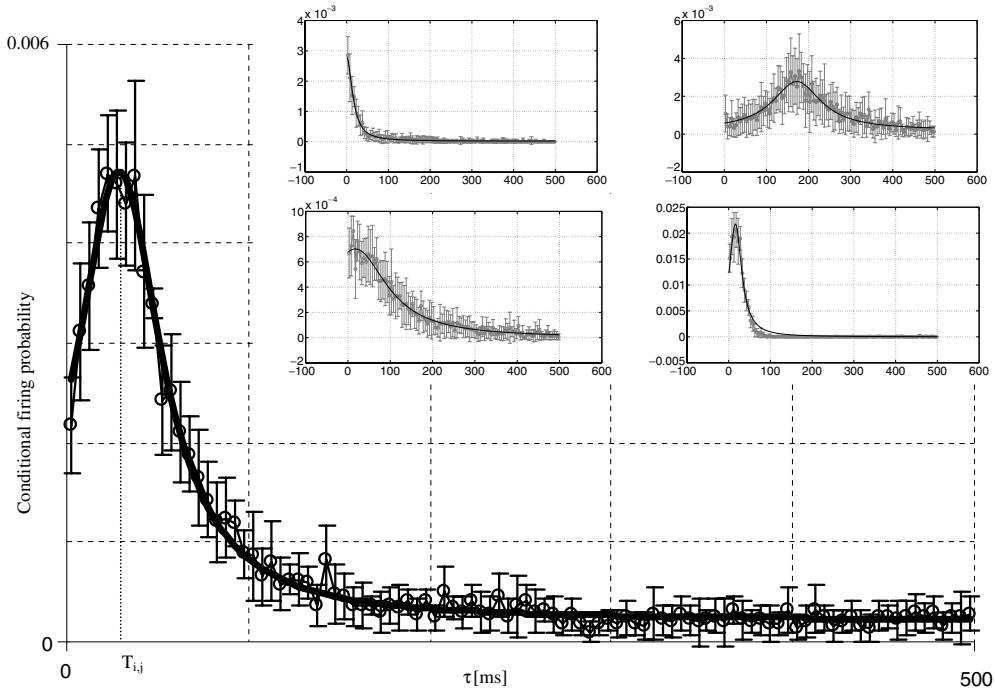

Figure 3. Example of conditional firing probability curve, calculated using equation (2). Fitting equation (5) yields maximum $\mathrm{CFP}^{\mathrm{fit}}$ ($M_{i,j} = 4.5 \times 10^{-3}$) and delay until this maximum ($T_{i,j} = 29$ ms). Means ± SD of ten consecutive values from 0.5 ms bins are shown, data were recorded at 10 DIV. The maximum probability may seem extremely small. However, this is the probability to record a spike in a 0.5 ms interval. In the figure above, the probability to record a spike at electrode j within 50 ms after an action potential at electrode i can be estimated as $\approx 2 \times 50 \times 0.004 = 0.4$. The inset shows four other examples of CFP curves, illustrating the wide variety in strength and delay. Note different vertical scales.

relationship was not detected because the decrease to baseline was too slow, leading to $w_{i,j} > 250$ ms. Infrequently (less than 1% of the observed curves), a CFP curve with two peaks occurred. These were averaged by our fit algorithm to a single peaked curve. A typical pattern observed in some relationships in one of the daily recordings (culture *D*) was a period of (close to) zero CFP between ≈150 and 250 ms. This 'dip' could not be fitted properly by equation (5). Instead, an offset was estimated that averaged all CFP values beyond the peak, including the dip. This hardly influenced the values of $M_{i,j}$ and $T_{i,j}$.

3.1. Number of active electrodes and relationships

The development of the number of active electrodes and the number of relationships in seven cultures is shown in figure 4. In cultures *I* (♦), *II* (○), *IV* (□), and to some extent also in cultures *C* (×), and *E*(◊), the number of active electrodes increased with time until 25 DIV. Beyond 25–30 DIV the number of active electrodes tended to stabilize in *I* and *II*. In *IV* the number of active electrodes decreased beyond 25 DIV. The number of relationships in these cultures (*N*, see equation (6)) increased with the number of active electrodes. *N* sometimes approached the square of the number of active electrodes, indicating that most pairs of active electrodes were related. On average ≈2/3 of all possible pairs were related. An exception was the period around 20 days *in vitro*, when in most cultures very few relationships could be identified. In cultures *III* (△), and *D* (+) the number of active electrodes showed some rather large fluctuations without a clear trend, as did the number of relationships.

Cultures *A* and *B* (*single day recordings*) had 25 ± 5 and 17 ± 3 active electrodes at 12 DIV and 8 DIV, respectively. *N* was 364 ± 112 in culture *A* and 232 ± 101 in *B* (means ± SD).

3.2. Stability of set of relationships

To investigate the stability of the set of relationships in the long-term recordings we consecutively used all data blocks as a reference to calculate similarity indices. Figure 5(a) shows an example of similarity indices, calculated using two different reference blocks; at 16 DIV, and 27 DIV. Similar graphs were obtained for all reference data blocks. These graphs were smoothed by a moving average filter and the interval around each reference in which at least 50% of the set of relations remained intact (int50) was determined. For each culture we calculated an average int50 for each day (i.e. we averaged the int50 values obtained using all reference blocks of that day). Mean int50 (±SD) for all cultures are shown in figure 5(b). Two-way analysis of variance showed that int50 depended significantly on both time and culture ($p < 0.01$). However, if the graphs of the individual cultures were normalized to their maximum, thus eliminating the influence of absolute values, int50 depended significantly on time ($p < 0.01$) but not on the culture ($p \geqslant 0.2$).

Around 20 DIV similarity indices decreased to ≈0 in all cultures, regardless of the reference used. In this

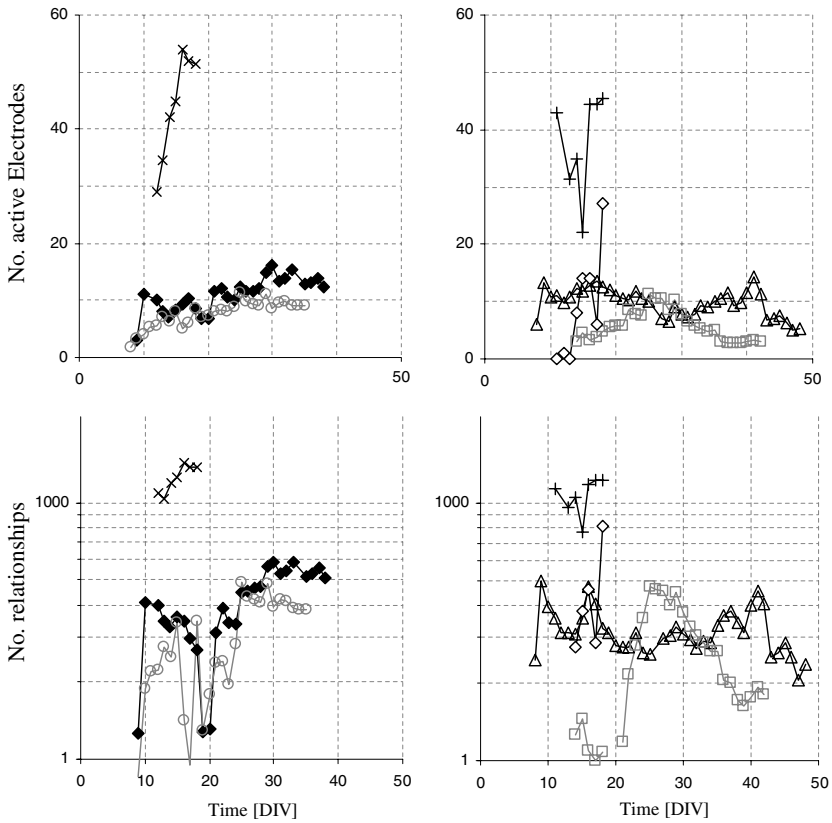

Figure 4. Development of the number of active electrodes and the number of relationships in seven cortical cultures. Measured data are divided into data blocks of ≈33 000 action potentials each. An electrode is considered active if it fires more than 250 times in a data block. Equation (5) is fitted to data from all pairs of active electrodes. An electrode pair (i, j) is considered related if $M_{i,j} \geqslant \text{offset}_{ij}$, 10 ms $\leqslant w_{i,j} \leqslant$ 250 ms and $T_{i,j} < 250$ ms. For clarity the number of active electrodes and the number of relationships were averaged per day. Left panel: ♦: culture *I*, ○: culture *II* and ×: culture *C*; right panel: △: culture *III*, □: culture *IV*, +: culture *D* and ◇: culture *E*.

period our analysis could reveal only a few relationships (see figure 4). However, a substantial part of the relationships that were found before 20 DIV were also identified in later data blocks in all cultures.

3.3. Relational strength and delay

Relationships differed widely in both strength and delay. $M_{i,j}$ ranged from 6×10^{-6} to 6.8×10^{-2} (approximately following a negative exponential distribution and averaging $(1.0 \pm 1.1) \times 10^{-3}$). We found $T_{i,j}$ values between 0 and 250 ms, more than 98% of which were below 100 ms.

3.3.1. Balanced sample test. We used a balanced sample test (see methods section) to investigate the stability per relationship over all data blocks recorded in 24 h. In this analysis we concentrated on relationships that were frequently found during 24 h. Figure 6 shows all relationships that were found in at least 50% of the 26 data blocks that were recorded during 24 h at 15 DIV and 29 DIV in culture *I*. At 29 DIV most relationships appeared quite stable as can be seen (figure 6(b)) from the standard deviations of $M_{i,j}$ and $T_{i,j}$. At 15 days *in vitro* (figure 6(a)), both $M_{i,j}$ and $T_{i,j}$ showed larger standard deviations, indicating larger fluctuations during those 24 h. Mean durations (±SD) of the data blocks were 53 ± 10 min and 57 ± 9 min, respectively. For readability the relationship indices in figure 6 are sorted such that $M_{i,j}$ and $T_{i,j}$ appear in decreasing order. Thus, the relationships are sorted differently for both traces. The bottom panels of figure 6 show how $M_{i,j}$ and $T_{i,j}$ are related. In all cultures, relationships with a long delay had a low maximum conditional firing probability, whereas 'faster' relationships varied in strength.

In the other long-term recordings, again we selected balanced samples to exclude differences caused by different duration of the data blocks. Only in culture *II* the average duration of data blocks differed slightly but significantly between both episodes (92 ± 19 min versus 107 ± 7 min), in the other cultures the difference was less than 8.7% and not significant (see table 1).

For each relationship in figure 6 the coefficient of variation was calculated, which gave an indication of the stability per relationship. These coefficients were averaged to give an impression of the overall stability of the network (see table 1).

Similar analysis was applied to cultures *A*, *B*, *C* and *D*. In cultures *A* and *B* we determined the mean coefficient of variation of $M_{i,j}$ (CV_M) and of $T_{i,j}$ (CV_T) at a single day only. In all other cultures CV_M was significantly lower in the later measurements (single tailed paired *t*-test: $p < 0.04$). CV_T decreased slightly as well, but not significantly. CV_M was always much smaller than CV_T. The results are summarized in table 1.

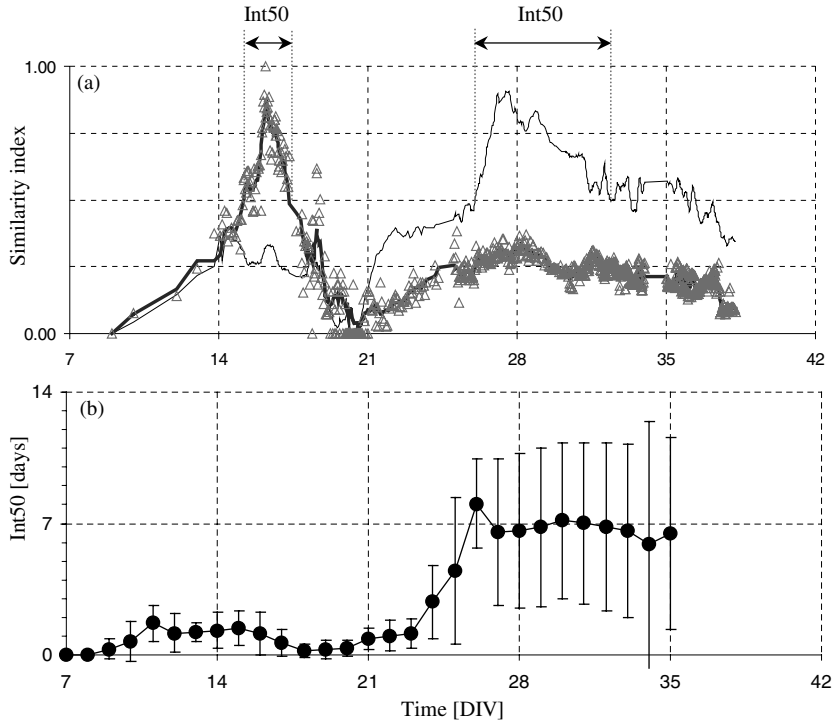

Figure 5. Stability of the set of relationships. A long-term recording was divided into 772 data blocks. Panel (a) shows a typical example of similarity indices (Si, equation (7)) for all data blocks calculated using two different reference blocks: 16 DIV (Δ), and 27 DIV (individual similarity indices not shown for clarity). After moving average filtering (bold line: 16 DIV; thin line: 27 DIV) we determined int50: the duration of the interval around each reference point, in which Si remained above 0.5 (50% of the sets of relations remained intact). Similar graphs were constructed with reference to all other data blocks. For each culture we averaged int50 per day to enable comparison between cultures. Panel (b) shows the averaged graph for all cultures. Standard deviations refer to differences between cultures. Beyond 35 DIV, in two or more cultures the 50% intact interval could not be determined because the end of the long-term recording was reached before Si dropped below 0.5. The increase beyond 25 DIV was significant.

Table 1. Mean coefficients of variation in eight cultures at different stages of development.

Culture	Time (DIV)	Block duration (minutes)	Mean CV_M (%)	Mean CV_T (%)	ΔCV_M	ΔCV_T
A	12		34	98		
B	8		27	97		
C	11	23 ± 3	14.1	58.1	−18%	−25%
	17	25 ± 2	11.6	43.7		
D	12	21 ± 17	68	84	−81%	−38%
	18	20 ± 2	13	52		
I	15	53.3 ± 10.0	30	149	−23%	−13%
	29	56.9 ± 8.6	23	129		
II	15	92 ± 19	53	127	−55%	+47%
	22	107 ± 7	24	187		
III	12	38.2 ± 2.6	36	222	−28%	−10%
	24	39.6 ± 2.0	26	199		
IV	15	72 ± 11	38	241	−29%	−38%
	29	70 ± 10	27	153		
Mean					−39 ± 24%*	−13 ± 32%

In six cultures mean coefficients of variation of relational strength (CV_M) and delay (CV_T) were calculated at different days (second column, DIV = days *in vitro*). Days were selected to minimize differences in average data block length (third column). A data block consisted of 2^{15} action potential events. Only in culture *II* data block lengths differed significantly. In cultures *C* and *D*, recordings spanned 2 h, in cultures *I–IV*, data were recorded continuously for 24 h. In all cultures CV_M decreased significantly (*right-tailed paired *t*-test: $p < 0.04$) with ageing, the average decrease in CV_T was not significant.

3.3.2. Continuous stability assessment. Next, we investigated the development of CV_M throughout the long-term recordings. We calculated CV_M from the set of relationships that were found in at least 50% of the data blocks of a series. This selection criterion included 54% of all repeatedly identified relationships to determine CV_M. Figure 7(a) shows

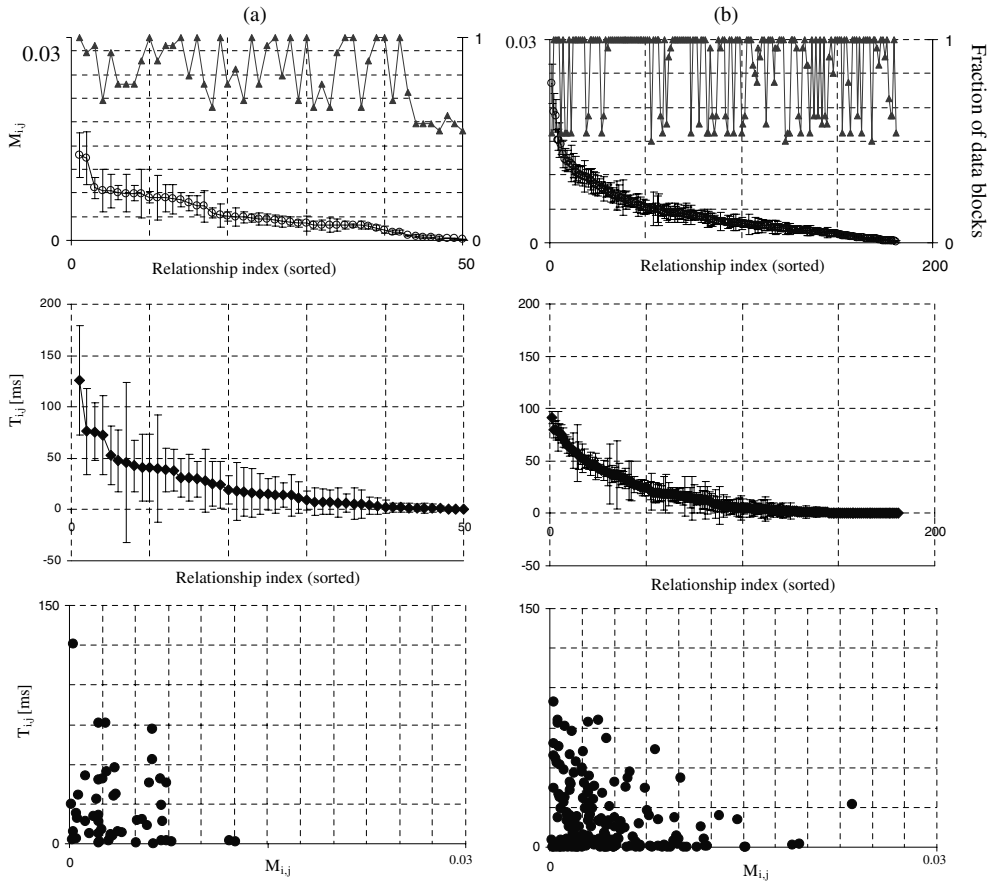

Figure 6. Mean strength and delay of all relations that were found in at least 50% of the data blocks recorded during 24 h in culture *I*. At 15 DIV (a) and 29 DIV (b), recorded data were divided into 26 data blocks. For all pairs of active electrodes (i, j) $M_{i,j}$ (upper traces, ○, left axis) and $T_{i,j}$ (middle traces) were calculated in each data block. Average values (±SD) of the selected relations are shown (fraction of data blocks depicted in upper traces, ▲, right axis). Relation indices are ordered such that both $M_{i,j}$ and $T_{i,j}$ are descending. Note that orders differ. The bottom panels relate average $M_{i,j}$ and $T_{i,j}$ for the identified relationships.

the decrease with time of the average coefficient of variation of M (CV_M) in a long-term recording, calculated over series of 15 consecutive data blocks. Similar curves were calculated for all long-term recordings. In three cultures the mean coefficient of variation showed some kind of plateau between 28 and 42 DIV, around 25% on average. In culture *II* there was higher fluctuation in the coefficient of variation. The mean coefficient of variation in most data blocks was also larger than in the other cultures, which may (partially) have been caused by the length of the data blocks, which were much larger in this culture (1.5 days on average, versus 0.4 ± 0.1 days in the other experiments). Pooled data of all cultures yielded a correlation coefficient $\rho = -0.32$, indicating that CV_M decreased with time. This correlation was significant ($p < 0.01$). Averaging CV_M of all cultures per week *in vitro* (WIV) yielded figure 7(b), which shows that CV_M decreased beyond the third week *in vitro*. From the decreasing standard deviation it can be seen that CV_M stabilized, at a level around 25%.

3.4. Development of relationships throughout long-term recordings

In four long-term recordings we found 253 pairs that were related in more than 25% of all data blocks. We investigated their development in time, which appeared quite gradual. For example, the strength of several of these relationships monotonously increased or decreased for more than a day (39 and 29 relationships, respectively). Relationships found in at least 10% of all data blocks (569) yielded even more such periods (69 and 59, respectively). However, the data points of some of these relationships were rather scattered, which sometimes complicated interpretation. Often, frequently found relationships were present predominantly in later data blocks (beyond 20–25 DIV). To study periods with high data point density, we focused on the relationships that could be identified in at least 50% of the data blocks recorded beyond 30 DIV (61 relationships in four cultures). Still, in most relationships $M_{i,j}$ developed rather gradually. Although it also showed fluctuations, we often observed periods of monotonous increase or decrease that lasted for a day or more. Figure 8 shows examples of the development of $M_{i,j}$ and $T_{i,j}$ of three relationships throughout a long-term recording. Three basic patterns were observed: some relationships showed a more or less constant $M_{i,j}$ value (33% of the relationships), in others $M_{i,j}$ increased (39%) or first increased and then decreased (28%). Of course this subdivision was rather arbitrary and several relationships could be classified into more than one category.

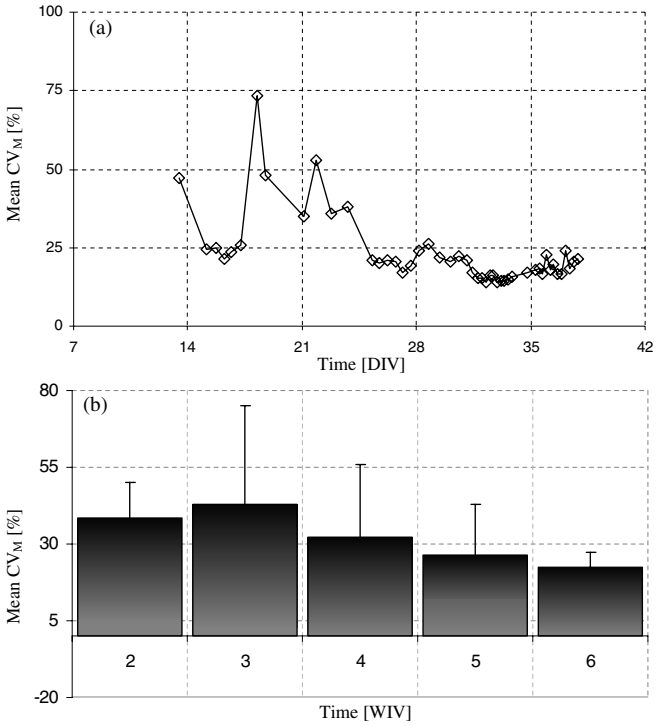

Figure 7. Development of the average coefficient of variation of relational strength. A long-term recording was divided into data blocks. In all data blocks M matrices were determined. Next, data blocks were grouped into series of 15 consecutive blocks. For the set of relationships that were found in at least 50% of the 15 blocks in a series, we calculated means and standard deviations of $M_{i,j}$ and the coefficients of variation ($100 \times$ SD/mean). These individual coefficients of variation were averaged to obtain CV_M. (a) Shows the development of CV_M in culture *I*. On average CV_M decreased with time. Pooled data of all cultures yielded a correlation coefficient $\rho = -0.32$. This correlation was significant ($p < 0.01$). (b) Shows mean CV_M of all cultures during the second to sixth week *in vitro* (WIV) to indicate the stabilization around 25% beyond the fourth week *in vitro*.

4. Discussion

Cortical networks were cultured on multi-electrode arrays (MEAs) to enable simultaneous measurement of signals from numerous electrodes. For all pairs (i, j) of active electrodes, we calculated the conditional firing probability $CFP_{i,j}[\tau]$. We investigated relationships between electrodes that recorded more than 250 spikes in a data block, which resulted in a number of active electrodes as shown in figure 4. Given the high cell density, a higher number of active electrodes might have been expected. However, the requirement of 250 action potentials excluded several electrodes that showed some ongoing activity but did not reach threshold, which decreased the number of active electrodes. Another factor that reduced this number was the small electrode size (10 μm) (used to promote single-unit recordings). Recent studies that used larger electrodes (30 μm) (with high probability for multi-unit recordings) and much lower 'active' thresholds (Chang *et al* 2006, Eytan and Marom 2006) found far more active electrodes. Our analysis emphasized the relationships between electrodes with high firing rates, and may have discarded relationships between electrodes that recorded less action potentials. However, on the roadmap of neuronal connections it gives a useful description of the highways.

Relationships were characterized by two parameters, $M_{i,j}$ and $T_{i,j}$, which were interpreted as measures for strength and delay of a relationship. We fitted equation (5) to the CFP curves to obtain values for these parameters. The applicability of this function is further discussed in the appendix. Two matrices M and T were constructed to describe the whole network. To assess the usability of the proposed method we examined the stability of these matrices during the development of cortical cultures.

4.1. Conditional firing probability is a cross-correlation related measure

Conditional firing probabilities were calculated using equation (2). Description of all signals by point processes enabled us to calculate the numerator as $\Sigma X_i[t] \cdot X_j[t + \tau]$, which led to a formula that resembled cross-correlation (equation (3)).

In equation (3), t and τ are time discrete variables and only the values $X[t] = 1$ may contribute to the summation. This means that the absolute maximum of $R[\tau]$ depends on the number of action potentials in X, which may differ widely between electrodes (Palm *et al* 1988). If the maximum of $R[\tau]$ is to be used as a measure for the strength of a relationship between two electrodes, this dependence should be corrected for. This problem has been addressed by several researchers and solutions have been proposed to compute a shuffle-corrected cross-correlogram (Palm *et al* 1988, Brody 1999), or to normalize to the number of action potentials in X_i or X_j. These measures have been described as 'effectiveness' and 'contribution', respectively, of which effectiveness (normalization to $\Sigma_t X_i[t]$) is easier to interpret (Aertsen and Gerstein 1985). This latter normalization leads to equation (2), emphasizing that conditional firing probability is a cross-correlation based measure.

Model studies showed that cross-correlation based analyses are far more sensitive to excitatory connections than to inhibitory ones (Aertsen and Gerstein 1985, Melssen and Epping 1987, Palm *et al* 1988), which may complicate a proper analysis. However, in cortical cultures only a small fraction (≈5–15%) of the neurons is inhibitory (Hayashi *et al* 2003, Wagenaar *et al* 2005b).

4.2. Deviating CFP curves

For all pairs of electrodes equation (5) was fitted to the CFP curves. This equation described the data adequately in a vast majority of the relationships. Occasionally we found a CFP curve with two separate peaks, indicating that the relationship between the two electrodes was actually based on more than one pathway. Fitting equation (5) resulted in an average of both peaks, and thus to an abstract description of the average effects of multiple pathways, just like it did in relationships that showed a single peak.

In one culture (culture *D*) we observed a dip in some of the CFP curves between 150 and 250 ms. The occurrence of such a pattern increased with ageing in this culture. This dip may

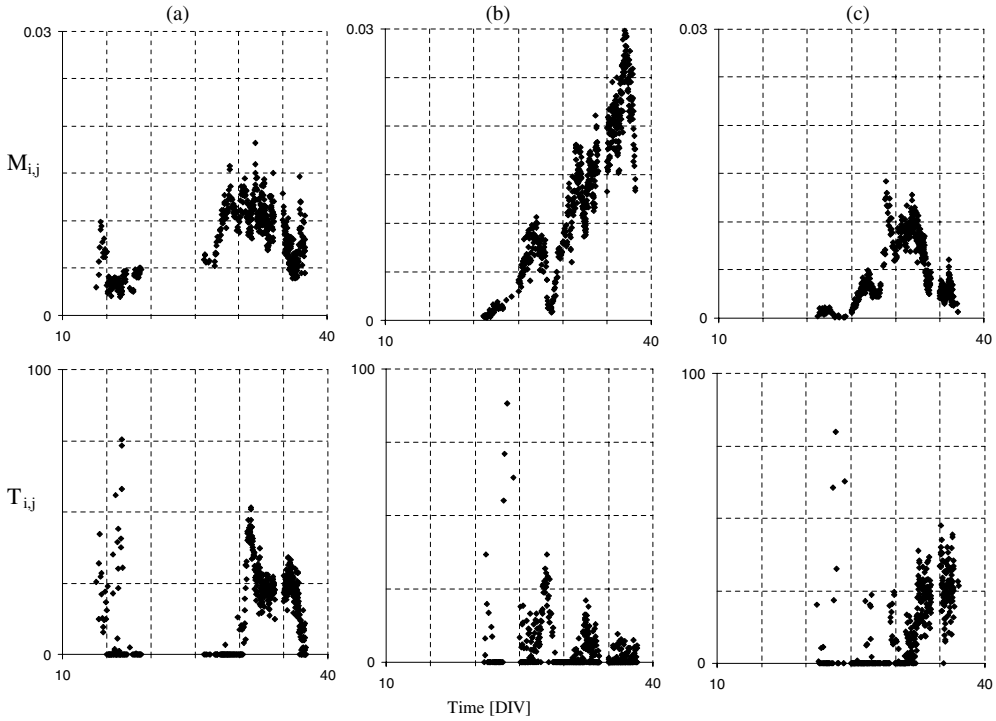

Figure 8. Examples of development of strength and delay of relations throughout long-term recordings. Sixty-one relations that were found in the last 50 data blocks of long-term recordings from four cultures were selected. The development of $M_{i,j}$ (upper panels) and $T_{i,j}$ (lower panels) of these relations between pairs of electrodes (i, j) was traced back throughout the long-term recording. The figure shows examples of three basic types of development: (a) shows a relation where $M_{i,j}$ fluctuates around a horizontal line (33% of the relations); (b) shows an increasing $M_{i,j}$ (39%) and in (c), $M_{i,j}$ increases first and then decreases (28%).

have been caused by activation of inhibitory neurons, which may have been present in higher numbers in this culture than in others. Still, in this culture the excitatory relationship was adequately described by equation (5) in terms of $M_{i,j}$ and $T_{i,j}$ (however, we obviously missed an interesting phenomenon in this culture). The low incidence of this 'dipped' pattern is probably explained by the relatively small fraction of inhibitory neurons and the low sensitivity of the method for inhibitory connections as discussed above.

4.3. Influence of surrounding network on relationships

Figure 6 illustrates that many relationships had low or zero delay. We did not pharmacologically determine whether or not short-latency relationships could have been caused by single cells in contact with multiple electrodes. Given the large distance between the electrodes (70 or 100 μm) it seems impossible that a soma made contact with more than one electrode. It might be possible that an electrode picked up signals from an axon from a soma connected to another electrode. However, experiments at NIN indicated that this is very unlikely (see van Pelt *et al* (2004b), p 2055). Thus, relationships between electrodes may reflect network characteristics: either causal activation or a shared common input.

In our analysis τ was restricted to a maximum of 500 ms to reduce computational load. It is possible that we missed relevant relationships with latencies longer than 500 ms. However, in most relationships the CFP curves had reached a stable level long before $\tau = 500$ ms (see figure 3), suggesting that an interval of 500 ms was usually long enough to analyze related pairs of electrodes. An exception may have been the period around 20 DIV, when in most cultures very few relationships were found. Our inability to identify relationships around 20 DIV may be explained by the average length of the bursts in this period, which exceeded 500 ms from ≈18 DIV until ≈24 DIV (van Pelt *et al* 2004a, 2004b). The number of excitatory connections that reaches a maximum in this period may have caused this long duration of network bursts. Excitatory connections may form loops, which means that an action potential in i will mostly be followed by (many) others, leading to (many) time shifted responses in a related electrode j and thus to a CFP curve with a less pronounced peak. Indeed, most CFP curves were flat or decreased too slowly to enable proper analysis over a 500 ms interval. Extension of the analysis interval (to 1, or even 2 s) yielded a larger number of relationships in the period around 20 DIV. Still, we decided to use a 500 ms analysis interval because such a long analysis interval highly increased the computational load, and only appeared useful around 20 DIV.

It is important to note that the relationships that we found did not solely depend on the pathways between each pair of electrodes, but were also influenced by the surrounding network. Most electrodes showed a peaked autocorrelation (at $\tau \neq 0$), as shown in figure 9. This suggests that these electrodes were part of an excitatory loop. If a spike at electrode i may be followed with an increased probability by another one at a

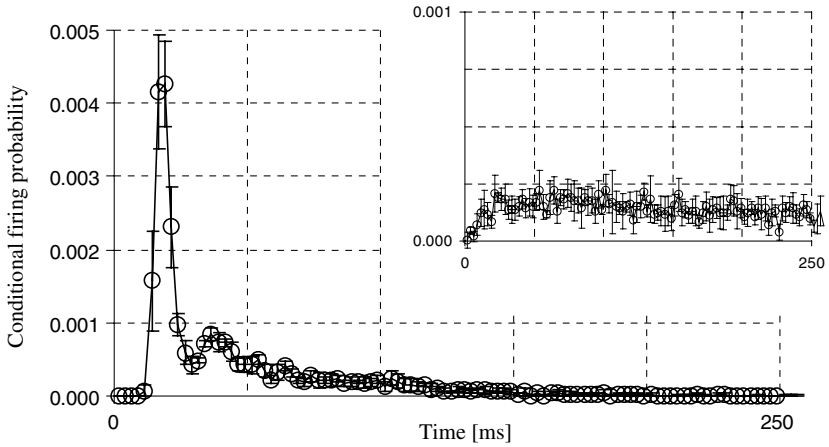

Figure 9. Example of conditional probability of a second action potential at electrode i at different delays, given that a first spike was recorded at $t = 0$. The curve was obtained with equation (2), by setting $i = j$. Each circle shows the mean value of five consecutive time bins (±SD). The peak at zero delay is one by definition because $N_{\text{follow}}[0] = N_i$ (see equations (1) and (2)). The figure shows an example of an electrode with an increased conditional firing probability around 15 ms. 80–90% of the electrodes showed such a pattern (delays varied). The inset shows an example of an electrode with a flat CFP (10–20%). Note that the vertical scales are different.

certain delay, it is likely that one or more neurons connected to i activate some part of the surrounding network, which again activates electrode i. Another possibility might be that i receives oscillatory input. However, this means that the neurons that provide this input are part of an excitatory loop. Alternatively, electrode i might receive input from another part of the network via two pathways with different latencies. This would also lead to a peak in the autocorrelation at $\tau \neq 0$. However, this would not explain the second, much lower peak seen in figure 9 at twice the delay of the first one. This second, smaller peak is to be expected if a neuron at electrode i is part of an excitatory loop. A fourth possibility might be the presence of the so-called pacemaker cells, which have been suggested in the cortex. However, it seems very unlikely that 80–90% of all cells that we recorded from are pacemaker cells. Thus, a peaked autocorrelation suggests an excitatory loop, either containing a recorded neuron or not. An excitatory loop may contain two or more neurons. Nakanishi and Kukita demonstrated bidirectional coupling between some pairs of neurons in cultured cortical networks using a whole cell current clamp technique (Nakanishi and Kukita 1998).

Excitatory loops do influence CFP curves. In a linear approximation, it has been suggested to calculate the deconvolution of the CFP curve and the autocorrelation in order to obtain a 'synaptic response function' (Eggermont 1990). 10–20% of all electrodes showed a flat autocorrelation, indicating that these electrodes were not cyclically activated. Relationships involving these electrodes had the same general shape as other relationships (figure 1), and could also be described by equation (5). Apparently, a repetitive pattern in the input signal did not alter the general shape of the CFP curve, only the parameter values were influenced. Because of the symmetry of the autocorrelation, a deconvolution would not affect $T_{i,j}$. Thus, delays found in this study would approach real latencies, whereas $M_{i,j}$ values would be affected. Existing pathways between a pair of electrodes may even remain undetected due to cyclic reactivation by excitatory loops. On the other hand, if a relationship is identified, this does indicate the existence of neuronal pathways between a pair of electrodes. Only the observed strengths and possibly latencies are influenced by the surrounding network.

4.4. Stability

In all cultures the similarity index decreased faster around reference points in the early days of measurement than around those in later recordings (see figure 5). On average int50 varied around one day in young cultures whereas beyond 25 DIV, it averaged around a week. This suggests that new relationships are formed or disappear more rapidly in younger cultures than in older ones, indicating that the networks stabilize with time. This was a rather general phenomenon as this increase with time was significant and did not depend significantly on the culture.

Relationships between active electrodes changed with time, possibly due to modulation of synaptic efficacy, or synaptogenesis. Movement of neurons might also cause a relationship to change. However, it seems unlikely that this would lead to gradual changes as seen in figure 8. Moreover, the set of active electrodes was quite stable, which seems improbable with substantial movement of cell bodies.

In three long-term recordings, the individual relationships between the electrodes stabilized after ≈4 weeks *in vitro* (e.g. see figure 7(a)). In culture *II*, coefficient of variation analysis did not show stabilization and the mean values remained higher. However, this culture showed less spontaneous activity, resulting in much longer lasting data blocks than in the other three experiments. Thus, a series of 15 consecutive blocks was spun out over a much longer time interval, which explained at least part of the larger variations per series.

Table 1 shows that coefficients of variation of T were very high. Still, figure 6(b) suggests that delays are quite stable in culture *I* at 29 DIV. The high coefficients of variation in table 1 were often caused by relationships with a mean delay close to 0 ms in which one or a few outliers led to

relatively large standard deviations. If there was more than one outlier, these were often closely clustered, possibly indicating activation of a second pathway. Sometimes $T_{i,j}$ was 0 at the beginning of an analysis interval and started to increase in the second half. In these cases a high coefficient of variation probably reflected developmental changes.

In general, we observed that after ≈4 weeks *in vitro*, the set of identified relationships remained stable (figure 5) and the individual relationships appeared quite stable in both strength and delay (see figures 6 and 7). This is in agreement with previous findings by Kamioka *et al* (1996) and a recent study by Chiappalone *et al* (2006). van Pelt *et al* concluded that the firing rate profiles within network bursts can change gradually over longer periods of development *in vitro*, although they are remarkably stable over periods of several days (van Pelt *et al* 2004b). In particular, they showed that network burst duration increased significantly up to the end of the third week *in vitro*, and decreased in the week thereafter. At the end of the fourth week *in vitro* the network burst firing rate profile stabilizes with very short risetime. Our analysis goes one step further; it enabled us to attribute the changes in network activity patterns to changing individual relationships between electrodes.

In conclusion, conditional firing probabilities provide usable descriptions of relationships between firing activities at electrode pairs in cultured neuronal networks. Despite the high variability seen in spontaneous network activity (Wagenaar *et al* 2006), the set of identified relationships stabilizes after ≈25 DIV and the individual relationships in such a set are quite stable in terms of relational strength and delay on a time scale of days. Our analysis revealed the quite stable underlying probabilistic structure of the network, which was possible only if large groups of action potentials were observed, far more than a single burst may contain. Individual spiking patterns varied widely in periods with very stable connectivity in terms of conditional firing probability.

High variability in spontaneous activity is one of the major problems in plasticity studies that aim to induce connectivity alterations by electrical stimulation. The induced changes will have to exceed spontaneous fluctuations. Our analysis provides a tool to investigate induced plasticity in detail whilst spontaneous fluctuations in the identified relationships are much smaller than those in spontaneous firing patterns.

Appendix

A vast majority of the relationships in all cultures could be adequately described by equation (5). The central limit theorem says that any sum of many independent identically distributed random variables with finite variance will be approximately normally distributed (Kallenberg 1997). Assuming that the functional connection between a pair of electrodes does not change during a data block, responses can be seen as a sum of identically distributed random variables. Thus, if many output spikes are taken into account a normal distribution may be assumed.

Equation (5) is a first-order approximation of a Gaussian distribution function:

$$P(x) = \frac{1}{\sigma\sqrt{2\pi}} \exp\left\{-\frac{(x-\mu_x)^2}{2\sigma^2}\right\}. \qquad \text{(A.1)}$$

Using the Taylor series expansion: $\exp(x) = \Sigma(x^n/n!)$ and its first-order approximation $\exp(x) \approx 1 + x$, and thus $\exp(-x) \approx 1/(1+x)$, equation (7) can be written as

$$P(x) \approx \frac{1}{\sigma\sqrt{2\pi}} \cdot \left\{\frac{1}{1+\left[\frac{x-\mu_x}{\sqrt{2}\sigma}\right]^2}\right\}. \qquad \text{(A.2)}$$

With $T_{i,j} = \mu_x$, $M_{i,j} = [\sigma \cdot \sqrt{(2\pi)}]^{-1}$ and $w_{i,j} = \sigma \cdot \sqrt{2}$, this results in equation (5). This would require $M_{i,j}$ to be equal to $(w_{i,j} \cdot \sqrt{\pi})^{-1}$. However, releasing the relation between $M_{i,j}$ and $w_{i,j}$ gives a higher degree of freedom to obtain better fits. It also allows the sum over $\tau(\Sigma_\tau \mathrm{CFP}_{i,j}[\tau])$ to deviate from 1, in contrast to common probability density functions. In most relations we found $\Sigma_\tau \mathrm{CFP}_{i,j}[\tau] < 1$, which was only partially caused by the limited interval $0 \leqslant \tau \leqslant 500$ ms. If the firing rate of neuron i is much higher than that of j, the probability that j will show an action potential in any limited interval after a spike in i is less than 1. If neuron j fires far more frequently than i, it is not unlikely that j will fire more than once in the 500 ms analysis interval, which may lead to $\Sigma_\tau \mathrm{CFP}_{i,j}[\tau] > 1$. In contrast to common probability density functions, here events are not mutually exclusive. Neuron j may fire at different delays after the spike in i. Indeed, occasionally we found relationships with $\Sigma_\tau \mathrm{CFP}_{i,j}[\tau] > 1$.

References

Aertsen A M H J and Gerstein G L 1985 Evaluation of neural connectivity: sensitivity of cross-correlation *Brain Res.* **340** 341–54

Brody C 1999 Correlations without synchrony *Neural Comput.* **11** 1537–51

Castellone P, Rutten W L C and Marani E 2003 Cross-interval histogram analysis of neuronal activity on multi-electrode arrays *IEEE EMBS Conf. on Neural Engineering (Capri Island, Italy)*

Chang J C, Brewer G J and Wheeler B C 2006 Neuronal network structuring induces greater neuronal activity through enhanced astroglial development *J. Neural Eng.* **3** 217–26

Chiappalone M, Bove M, Vato A, Tedesco M and Martinoia S 2006 Dissociated cortical networks show spontaneously correlated activity patterns during *in vitro* development *Brain Res.* **1093** 41–53

Eggermont J J 1990 *The Correlative Brain* (Tuebingen: Springer)

Eytan D, Brenner N and Marom S 2003 Selective adaptation in networks of cortical neurons *J. Neurosci.* **23** 9349–56

Eytan D and Marom S 2006 Dynamics and effective topology underlying synchronization in networks of cortical neurons *J. Neurosci.* **26** 8465–76

Eytan D, Minerbi A, Ziv N and Marom S 2004 Dopamine-induced dispersion of correlations between action potentials in networks of cortical neurons *J. Neurophysiol.* **92** 1817–24

Gross G W, Harsch A, Rhoades B K and Goepel W 1997 Odor, drug and toxin analysis with neuronal networks *in vitro*: extracellular array recording of network responses *Biosensors Bioelectron.* **12** 373–93

Gross G W, Rhoades B K, Azzazy H M E and Wu M C 1995 The use of neuronal networks on multielectrode arrays as biosensors *Biosensors Bioelectron.* **10** 553–67

Hayashi K, Kawai-Hirai R, Harada A and Takata K 2003 Inhibitory neurons from fetal rat cerebral cortex exert delayed axon formation and active migration *in vitro J. Cell Sci.* **116** 4419–28

Jimbo Y, Kawana A, Parodi P and Torre V 2000 The dynamics of a neuronal culture of dissociated cortical neurons of neonatal rats *Biol. Cybern.* **83** 1–20

Jimbo Y and Robinson H 2000 Propagation of spontaneoussynchronized activity in cortical slice cultures recorded by planar electrode arrays *Bioelectrochemistry* **51** 107–15

Jimbo Y, Robinson H P C and Kawana A 1998 Strengthening of synchronized activity by tetanic stimulation in cortical cultures: application of planar electrode arrays *IEEE Trans. Biomed. Eng.* **45** 1297–304

Jimbo Y, Tateno T and Robinson H 1999 Simultaneous induction of pathway-specific potentiation and depression in networks of cortical neurons *Biophys. J.* **76** 670–8

Kallenberg O 1997 *Foundations of Modern Probability* (New York: Springer)

Kamioka H, Maeda E, Jimbo Y, Robinson H P C and Kawana A 1996 Spontaneous periodic synchronized bursting during formation of mature patterns of connections in cortical cultures *Neurosci. Lett.* **206** 109–12

Madhavan R, Chao Z C and Potter S M 2005 Spontaneous bursts are better indicators of tetanus-induced plasticity than responses to probe stimuli *IEEE EMBS 2nd Neural Eng. Conf. (Arlington, VA)*

Marom S and Eytan D 2004 Learning in *ex-vivo* developing networks of cortical neurons *Prog. Brain Res.* **147** 189–99

Marom S and Shahaf G 2002 Development, learning and memory in large random networks of cortical neurones: lessons beyond anatomy *Q. Rev. Biophys.* **35** 63–87

Melssen W J and Epping W J M 1987 Detection and estimation of neural connectivity based on crosscorrelation analysis *Biol. Cybern.* **57** 403–14

Nakanishi K and Kukita F 1998 Functional synapses in synchronized bursting of neocortical neurons in culture *Brain Res.* **795** 137–46

Nelder J A and Mead R 1965 A simplex method for function minimization *Comput. J.* **7** 308–13

Palm G, Aertsen A M H J and Gerstein G L 1988 On the significance of correlation among neural spike trains *Biol. Cybern.* **59** 1–11

Ruaro M E, Bonifazi P and Torre V 2005 Towards the neurocomputer: image processing and pattern recognition with neuronal cultures *IEEE Trans. Biomed. Eng.* **52** 371–83

Shahaf G and Marom S 2001 Learning in networks of cortical neurons *J. Neurosci.* **21** 8782–8

Tal D, Jacobson E, Lyakhov V and Marom S 2001 Frequency tuning of input-output relation in a rat cortical neuron *in-vitro Neurosci. Lett.* **300** 21–4

Tam D C 2001 A spike train analysis for correlating burst firings in neurons *Neurocomputing* **38–40** 951–5

Tateno T, Kawana A and Jimbo Y 2002 Analytical characterization of spontaneous firing in networks of developing rat cultured cortical neurons *Phys. Rev.* E **65** 051924

van Pelt J, Corner M A, Wolters P S, Rutten W L C and Ramakers G J 2004a Longterm stability and developmental changes in spontaneous network burst firing patterns in dissociated rat cerebral cortex cell cultures on multielectrode arrays *Neurosci. Lett.* **361** 86–9

van Pelt J, Wolters P S, Corner M A, Rutten W L C and Ramakers G J 2004b Long-term characterization of firing dynamics of spontaneous bursts in cultured neural networks *IEEE Trans. Biomed. Eng.* **51** 2051–62

Wagenaar D A, Demarse T B and Potter S M 2005a MeaBench: A toolset for multi-electrode data acquisition and on-line analysis *2nd Int. IEEE EMBS Conf. on Neural Engineering (Arlington, VA)*

Wagenaar D A, Madhavan R, Pine J and Potter S M 2005b Controlling bursting in cortical cultures with closed-loop multi-electrode stimulation *J. Neurosci.* **25** 680–8

Wagenaar D A, Pine J and Potter S M 2006 An extremely rich repertoire of bursting patterns during the development of cortical cultures *BMC Neurosci.* **7** 11